molbank

MDPI

Short Note

3-Isobutyl-5,5,7-tris(3-methylbut-2-en-1-yl)-1-phenyl-1,7-dihydro-4*H*-indazole-4,6(5*H*)-dione

José Edmilson Ribeiro do Nascimento, Daniela Hartwig, Raquel Guimarães Jacob * and Márcio Santos Silva *

Laboratório de Síntese Orgânica Limpa–LASOL, CCQFA, Universidade Federal de Pelotas–UFPel, P.O. Box 354, Pelotas 96010-900, RS, Brazil; jedmilsonrn@gmail.com (J.E.R.d.N.); dani.hartwig@gmail.com (D.H.)
* Correspondence: raquel.jacob@ufpel.edu.br (R.G.J.); silva.ms@ufpel.edu.br (M.S.S.)

Abstract: Here we describe the functionalization of lupulone natural compound in obtaining 3-Isobutyl-5,5,7-tris(3-methylbut-2-en-1-yl)-1-phenyl-1,7-dihydro-4*H*-indazole-4,6(5*H*)-dione. The lupulone-*H*-indazole derivative was prepared with 75% yield through the reaction between lupulone and phenyl-hydrazine employing $SiO_2/ZnCl_2$ (30% *m*/*m*) as a support solid in a solvent-free condition. Based on the possibilities of products, a complete NMR structural characterization of this lupulone-*H*-indazole was performed by ^{1}H, $^{13}C\{^{1}H\}$, COSY, HSQC and HMBC NMR experiments, showing an important contribution in producing the first results related to lupulone reactivity.

Keywords: soft resin; lupulone-indazole; NMR Spectroscopy; solvent-free

Citation: Nascimento, J.E.R.d.; Hartwig, D.; Jacob, R.G.; Silva, M.S. 3-Isobutyl-5,5,7-tris(3-methylbut-2-en-1-yl)-1-phenyl-1,7-dihydro-4*H*-indazole-4,6(5*H*)-dione. *Molbank* **2022**, *2022*, M1330. https://doi.org/10.3390/M1330

Academic Editors: Stefano D'Errico and Annalisa Guaragna

Received: 29 December 2021
Accepted: 29 January 2022
Published: 1 February 2022

1. Introduction

Biomass is renewable organic material that comes from animals and plants [1]. These materials are getting the attention of researchers due to the chemical transformation ability, which can lead to molecules with therapeutic potential or great industrial applicability [1,2].

Humulus lupulus L. has long been used as a medicinal plant, and its benefits include blood purification, treatment of inflammation, and sedative properties [3]. The compounds present in the extracts or essential oil of this plant have also been explored regarding their synthetic potential [4].

Hop is a base material in the brewing process to provide flavor and aroma to beer. Hop essential oil is present in the glandular cells of the hop plant, *Humulus lupulus* (Cannabinaceae) [5]. Among the vast number of natural compounds in the hop extract [6] are humulone and lupulone (Figure 1), which exhibit biological activity against some human cancer cells and have antibiofilm properties [7,8].

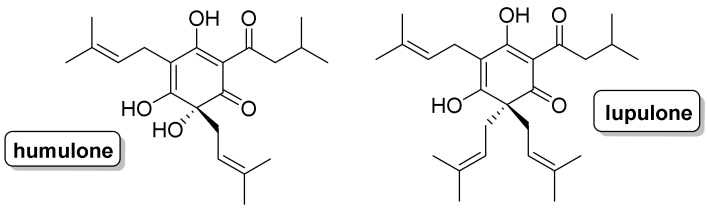

Figure 1. Structures of (−)-humulone and lupulone.

Based on our interest in the evaluation of the pharmacological properties of natural products [9,10], especially structural modification [11–14], we isolated lupulone from the hop plant. In this sense, the derivation of lupulone containing heterocyclic nitrogen represents a consolidated strategy to improve the pharmacological properties [11].

On the basis of these recent findings, we report here the first results related to the derivatization of lupulone through reaction with phenyl-hydrazine. Considering the lupulone structure and the possibilities of products, a full structural characterization was

performed, which confirmed the formation of a *H*-indazole ring through ^{1}H, $^{13}C\{^{1}H\}$, COSY, HSQC, and HMBC NMR experiments.

2. Results and Discussion

Lupulone was isolated from soft resin fraction of hops in a 3% (*m*/*m*) yield after extraction and chromatographic purification, according to Taniguchi's method [15,16]. The 3-Isobutyl-5,5,7-tris(3-methylbut-2-en-1-yl)-1-phenyl-1,7-dihydro-4*H*-indazole-4,6(5*H*)-dione was obtained through a solvent-free reaction under conventional heating between lupulone and phenyl-hydrazine, in the presence of $SiO_2/ZnCl_2$ (30% *m*/*m*) solid support [17]. After chromatographic purification of the crude, the lupulone derivative **4** was isolated in a moderate yield (75%). The structure of the lupulone derivative **4** was supported by 1D and 2D NMR experiments and HRMS analysis, as can be seen in the characterization data (Section 3: Materials and Methods).

Initially, the reaction between lupulone and phenyl-hydrazine was optimized. As seen in Table 1, the presence of an acid support solid was essential to produce the lupulone derivative, as the presence of the reagents only was not sufficient to detect a product. The heating of the reaction media increased the yield, with the use of 60 °C demonstrating the best performance (Table 1, entry 5). When an excess of phenyl-hydrazine was employed, the yield increased to 75% (Table 1, entry 6), although continuing to increase the amount of the phenyl-hydrazine did not enhance the reaction efficiency (Table 1, entry 6). The product highlighted in the Table 1 is the expected product in this functionalization.

Table 1. Optimization of the reaction between lupulone and phenyl-hydrazine.

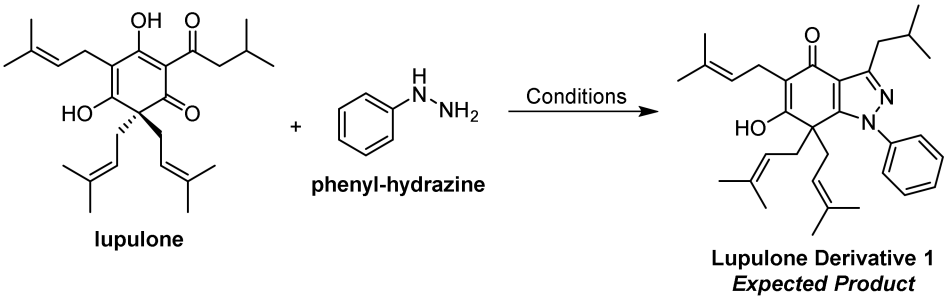

Entry	Catalyst (56 mol %)	Lupulone: Hydrazine Ratio (mmol)	Temp. (°C)	Yield (%) [a]
1	–	(0.5:0.5)	60	–
2	$SiO_2/ZnCl_2$	(0.5:0.5)	60	51
3	$SiO_2/ZnCl_2$	(0.5:0.5)	25	20
4	$SiO_2/ZnCl_2$	(0.5:0.5)	100	31
5	$SiO_2/ZnCl_2$	(0.5:0.6)	60	75
6	$SiO_2/ZnCl_2$	(0.5:0.7)	60	76

[a] Yield of the isolated product.

At this moment, the main product was isolated by column chromatography; however, several small by-products were also detected by thin-layer-chromatography of the crude reaction. Evaluation using mass spectrometry showed it was not possible to discriminate the product possibilities, because of mass similarities and the tautomerism effect (Figure 2). Additionally, when employing ^{1}H and $^{13}C\{^{1}H\}$ NMR experiments, it was possible to eliminate the lupulone derivatives **1**, **2**, and **5** (Figure 2), due the amount of aliphatic carbons, but this was not sufficient to clarify the lupulone derivatives **3**, **4** and **6** (see Figure 2). Thus, a full assignment was performed, for which 2D NMR experiments were also necessary. Based on this structural elucidation, COSY, HSQC and HMBC NMR experiments were carried out, and the NMR data were interpreted according to the Table 2.

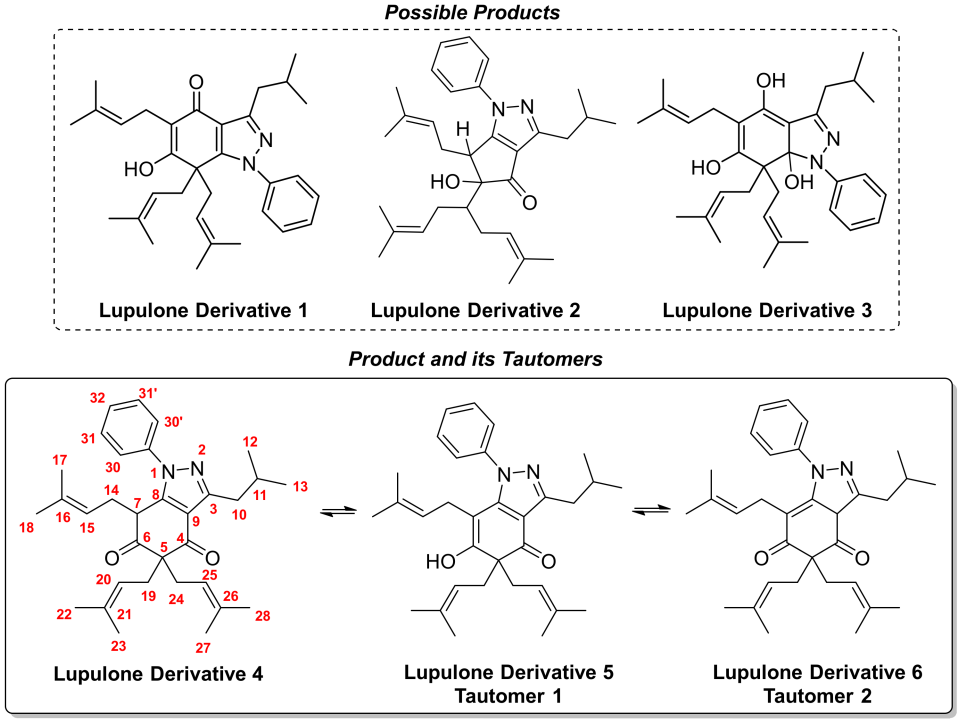

Figure 2. Possible products and full structural assignment of the lupulone derivative **4**.

Table 2. ^{1}H and ^{13}C chemical shifts, coupling constants, and HMBC 2D correlations of lupulone derivative **4**.

Number	^{1}H (ppm)	^{13}C (ppm)	^{1}H-^{13}C HMBC
1	—	—	—
2	—	—	—
3	—	153.6	—
4	—	193.1	—
5	—	65.7	—
6	—	210.0	—
7	3.89 (*dd*, *J* = 5.0 and 6.3 Hz)	46.8	6, 8, 9 and 14
8	—	147.1	—
9	—	118.6	—
10	2.98 (*d*, *J* = 7.2 Hz)	36.3	3 and 9
11	2.25 (*n*, *J* = 6.7 Hz)	28.1	3, 10, 12 and 13
12	1.07 (*d*, *J* = 6.7 Hz)	22.4	10 and 11
13	1.06 (*d*, *J* = 6.7 Hz)	22.3	10 and 11
14	2.10 (*ddd*, *J* = 6.3, 6.6 and 14.7 Hz)	30.1	6, 7, 8, 15 and 16
14′	2.55–2.70 (*m*)	30.1	6, 7, 8, 15 and 16
15	4.60 (*t*, *J* = 7.3 Hz)	118.4	14, 17 and 18
16	—	135.6	—
17	1.26 (s)	25.7	15 and 16
18	1.53 (s)	17.4	15 and 16
19	2.78 (*d*, *J* = 7.4 Hz)	33.9	4, 5, 6, 20 and 21
20	4.93 (*t*, *J* = 7.4 Hz)	118.1	19, 22 and 23
21	—	134.4	—
22	1.66 (*s*)	26.0	19, 20 and 21
23	1.72 (*s*)	18.0	19, 20 and 21
24	2.55–2.70 (*m*)	39.5	4, 5, 6, 25 and 26
25	4.94 (*t*, *J* = 7.3 Hz)	118.6	24, 27 and 28
26	—	135.1	—
27	1.53 (*s*)	25.9	24, 25 and 26

Table 2. *Cont.*

Number	^{1}H (ppm)	^{13}C (ppm)	^{1}H-^{13}C HMBC
28	1.67 (*s*)	17.7	24, 25 and 26
29	—	139.2	—
30	7.48–7.50 (*m*)	124.6	29 and 32
31	7.57–7.59 (*m*)	129.6	29
32	7.53–7.54 (*m*)	128.7	30

The 2D NMR experiments confirmed the formation of the *H*-indazole ring, according to the structural assignment (Figure 2). First, the ^{1}H spectrum (Figure S1) demonstrates a clear signal profile, with the aliphatic protons being easily identified (Table 2, methyl groups, numbers: 12, 13, 17, 18, 22, 23, 27 and 28), as well as the aromatic protons (Table 2, numbers 30, 31, 31′, 32). In a downfield ^{1}H chemical shift, it is possible to detect the vinylic signals (Table 2, numbers 15, 20 and 25) alongside an additional proton, established by integral values. This extra ^{1}H NMR signal in 3.9 ppm demonstrates a deshielded chemical shift due the proximity to nitrogen and carbonyl groups, or it could be derived from some hydroxyl group of the lupulone derivative **3** [18]. In a upfield region, it is possible to observe the aliphatic signals, considering the multiplicity standard (Table 2, numbers 10, 11, 14, 19 and 24). It is noteworthy that the protons 14 are diastereotopics with a distinct multiplicity profile (Table 2, numbers 14 and 14′, confirmed by HSQC), indicating the lupulone derivative **4** or its tautomer, with the lupulone derivative **6** as the possible product, due the presence of the aromatic ring near to these protons, which results in an anisotropic environment. Based on the COSY experiment, stronger correlations were observed between the protons 14 and 14′ with the deshielded aliphatic proton (number 7), which confirms the lupulone derivative **4** and excludes the lupulone derivative **6**.

According to the ^{13}C{^{1}H} spectrum (Figure S2), all 32 carbons can be visualized once no overlapping of signals occurred. The amount of aliphatic carbons corroborates with the *H*-indazole ring through the presence of an additional aliphatic carbon, differently from other probable products (Figure 2: lupulone derivatives **1**, **2** and **5**). Considering the aromatic region, only two downfield carbons are evident with a typical carbonyl chemical shift profile (Table 2, numbers 4 and 6, 193.0 and 209.9 ppm, respectively, confirmed by HMBC), which allows us to discard the lupulone derivative **3** due to the presence of phenol groups in the main structure [18]. Additionally, the *ortho* and *meta* carbons can be identified from aromatic ring based on the signal intensity. However, no further identifications could be evidenced without the HSQC and HMBC 2D NMR experiments (see NMR spectra in SI).

Although the ^{1}H and ^{13}C NMR profile can provide good evidence for the lupulone derivative **4** (Figure 2), more proof is necessary to confirm the main structure. Thus, a full structural elucidation is necessary to identify all protons and carbons signals, and for this purpose, 2D NMR experiments were carried out. As can be seen in Table 2, proton-carbon correlations are valuable for recognizing all NMR signals. Additionally, interpreting the COSY NMR experiment (Figure 3), the methyl groups 12 and 13 and the proton 10 were identified by the correlation with proton 11 (2.25 ppm, nonet) containing eight neighbor protons. In the same NMR region, the diastereotopic protons 14 and 14′ could be detected by the correlation between them and by a weak correlation with the vinylic proton 15, also confirming the methyl groups 17 and 18. The other two butene groups were recognized by the same correlation pattern, although no distinction among these groups was possible.

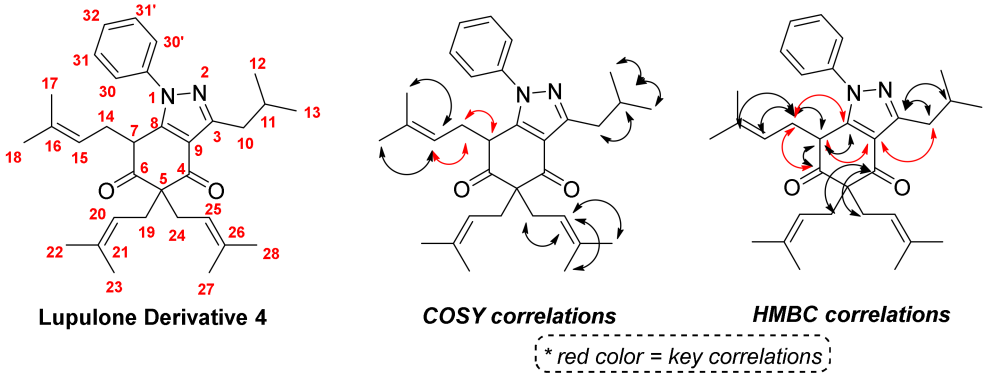

Figure 3. COSY and HMBC correlations in the lupulone derivative **4**.

Next, the HSQC NMR spectrum was evaluated (Figure S4). Based on the identification of the protons using proton–proton correlations, the carbons directly attached were detected. The aliphatic moiety was easily recognized, because there is only one quaternary carbon (Table 2, number 5). When the downfield region was checked, the vinylic carbons attached to the protons were identified (Table 2, numbers 15, 20 and 25) as were the *ortho*, *meta* and *para* carbons in the aromatic ring (Table 2, number 30, 31 and 32).

Finally, the HMBC NMR experiment was carried out to assign the quaternary carbons, confirming the main core of the lupulone derivative **4** (Figures S5–S7). In this way, to carry out the ^{1}H-^{13}C HMBC experiment, 10 Hz was used for the long-distance parameter (SI, CNST13), although this long-range term could be optimized for a proper assignment. Based on the proximity of protons and carbons, especially considering the stronger $^{3}J_{1H\text{-}13C}$ scalar coupling, the quaternary carbons were assigned. It is important to mention that the correlation between the diastereotopic protons 14 and 14′ and the carbons C6, C7, C8, C15 and C16 were also visualized in the HMBC NMR spectrum.

Analysis of HMBC NMR spectrum in the downfield region supports the formation of the lupulone derivative **4** (Figure 3). The quaternary carbon 3 was assigned by correlations with the protons 10 and 11, corroborating the typical ^{13}C chemical shift (Table 2; number 3; 153.6 ppm). The carbon 4 (carbonyl) can be confirmed by ^{3}J correlation with the protons 24 and 19 (Figure S7), but it does not have a correlation with the proton 7. The quaternary carbon-5 does not demonstrate correlation with the proton 7, which supports the lupulone derivative **4**. The carbon 6 demonstrates a similar profile with the ^{3}J correlation with the protons 7, 19 and 24. When we evaluated the carbon 7, only weak correlations were observed with the diastereotopic protons 14 and 14′. The carbon 8 was clearly assigned by the correlation with the proton 7 and a weak correlation with the diastereotopic protons 14 and 14′ (Figure S6). Finally, the carbon 9 was assigned by the correlations with the protons 7 and 10 (Figure 3).

The NMR experimental data completely support the lupulone derivative **4**. Although the possible tautomers of lupulone derivative **4** (Figure 2; tautomers 1 and 2) can change the chemical shift profile, their structures were not detected in the NMR spectra. Thus, to improve the discussion regarding the reactivity of the lupulone starting material, we propose a plausible mechanism (Figure 4) [19]. Initially, a keto-enol tautomerism justifies the formation of an aliphatic carbon in the main structure. The first step is the formation of imine from the reaction between ketone and amine organic functions, eliminating a water molecule. Afterward, a cyclization is favored, derived from the proximity between carbonyl and amine groups, followed by the elimination of the hydroxyl group (E1cB type). Finally, the base present in the media provides the formation of another carbonyl group, establishing the *H*-indazole ring and producing another water molecule. The formation of a heteroaromatic ring by the tautomerism effect affords the product lupulone derivative **4**, probably derived from the stability gain by the aromaticity (Figure 4). In addition, the lupulone derivative **2** was not observed; however, the ring contraction is a possible pathway, derived from an isomerization process [20]. Based on this mechanism, it is possible to

visualize the formation of various other products derived from the different pathways in this reaction (Figure S8, lupulone derivatives **1** and **3**), justifying the need to perform a full structural assignment, as varying the reaction conditions could produce distinct products.

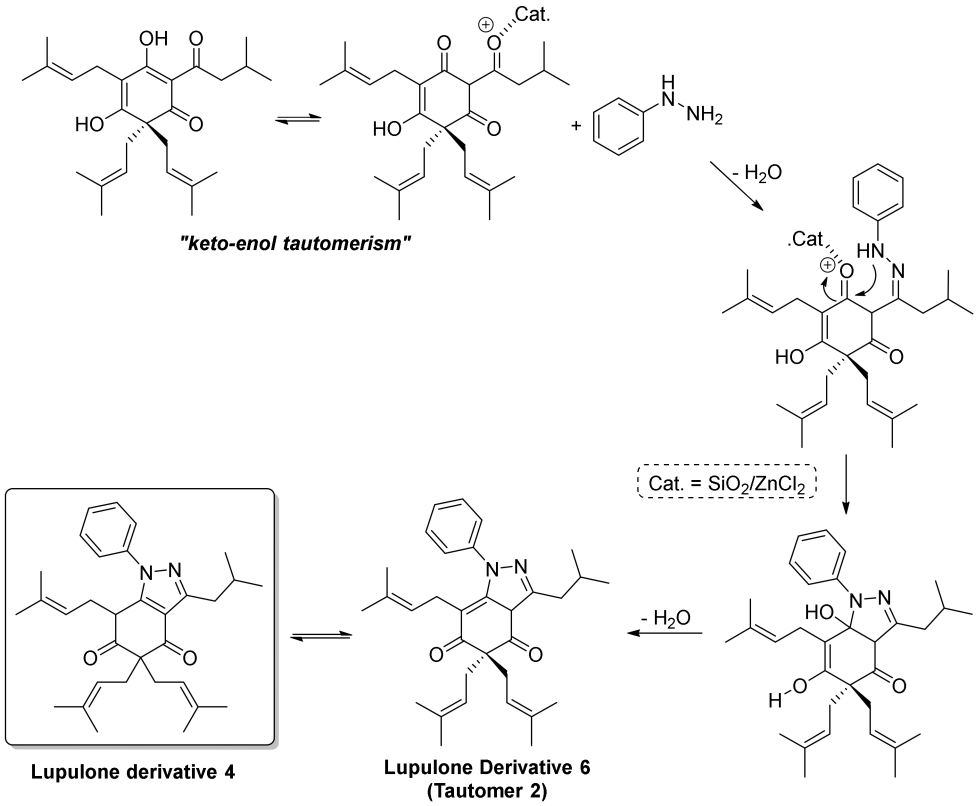

Figure 4. A plausible mechanism to obtain the lupulone derivative **4**.

3. Materials and Methods

The reactions were monitored by TLC carried out on pre-coated TLC sheets ALUGRAM® Xtra SIL G/UV_{254} by using UV light as the visualization agent and the mixture of 5% vanillin in 10% H_2SO_4 under heating conditions as the developing agent. Silica gel (particle size 63–200 μm) was used for flash chromatography. The reagents, solvents and chromatographic materials were purchased from Sigma-Aldrich® Brazil. The nuclear magnetic resonance (NMR) data were collected on a Bruker Avance III HD spectrometer (Bruker®, Atibaia, Brazil) operating at 400.0 MHz for ^{1}H and 100 MHz for ^{13}C. NMR data were recorded at 25 °C, with chemical shifts δ reported in parts per million and coupling constants J in Hertz. The NMR sample was prepared employing 5 mg of the respective lupulone derivative **4** in 600 μL deuterated chloroform. Chemical shifts of ^{1}H and ^{13}C{^{1}H} NMR experiments were referenced by TMS (tetramethylsilane) at δ = 0.0 ppm. Two-dimensional NMR experiments COSY, HSQC, and HMBC were performed using the standard Bruker pulse sequence with gradient. The relaxation delay, 90° pulse, spectral width, and number of data points for ^{1}H NMR were 1 s, 9.43 μs, 5580 Hz, and 64 K, respectively. The corresponding parameters for the ^{13}C NMR experiments were 0.5 s, 10.0 μs, 26,041 Hz, and 64 K, respectively. Two-dimensional experiments, including COSY, HSQC, and HMBC, were performed with 4 K × 512 (*t2* × *t1*) data points. The long-range coupling time for ^{1}H-^{13}C HMBC was 10 Hz. All data were analyzed using Bruker software (Topspin 3.6, Bruker®, Atibaia, Brazil). Low-resolution mass spectra (MS) were obtained with a Shimadzu GC-MS-QP2010 mass spectrometer (São Paulo, Brazil). The HRMS analyses were performed in a Bruker micrOTOF-QII spectrometer equipped with an APCI source operating in positive mode. The samples were solubilized in acetonitrile and analyzed by direct infusion at a constant flow rate of 180 μL/min. The acquisition parameters were capillary: 4000 V, end plate offset:

−500 V, nebulizer: 1.5 bar, dry gas: 1.5 L min^{-1}, and dry heater: 180 °C. The collision cell energy was set to 5.0 eV. The mass-to-charge ratio (m/z) data were processed and analyzed using Bruker Daltonics software: Compass Data Analysis and Isotope Pattern.

Experimental Procedure to obtain the Lupulone Derivative **4**: The 3-Isobutyl-5,5,7-tris(3-methylbut-2-en-1-yl)-1-phenyl-1,7-dihydro-4*H*-indazole-4,6(5*H*)-dione was obtained through the reaction between lupulone (0.5 mmol) and phenyl-hydrazine (0.6 mmol) employing 20 mg (0.277 mmol) of $SiO_2/ZnCl_2$ (30% m/m) [17] as a support solid in a solvent-free condition. The reaction media was heated to 60 °C for 20 h. The conventional heating was removed and the heterogenous catalyst was filtred using a small amount of ethyl acetate (2.0 mL). Then, the solvent was removed without an extraction step, and the sample obtained was directly purified by column chromatography. The lupulone derivative **4** was isolated in a moderate yield (75%) by column chromatography, employing a mixture of *n*-hexane/ethyl acetate in a 94:04 ratio. The product is a yellow oil with a pleasant smell.

Lupulone Derivative **4** Characterization: Yield 75%, yellow oil. NMR ^1H ($CDCl_3$, 400 MHz) δ 0.98 (d, J = 3.0 Hz, 3H), 0.99 (d, J = 3.0 Hz, 3H), 1.18 (s, 3H), 1.44 (s, 3H), 1.53 (s, 3H); 1.57 (m, 6H); 1.63 (s, 3H); 2.10 (*ddd*, J = 6.3, 6.6 and 14.7 Hz), 2.13–2.18 (m, 1H), 2.50–2.60 (m, 3H), 2.70 (d, J = 7.3 Hz, 2H), 2.90 (d, J = 7.2 Hz, 2H), 3.84–3.79 (m, 1H), 4.51 (t, J = 7.2 Hz, 1H), 4.86 (t, J = 7.3 Hz, 2H), 7.47–7.37 (m, 3H), 7.55–7.47 (m, 2H). ^{13}C NMR (100 MHz, $CDCl_3$) δ 17.36; 17.69; 17.96; 22.34; 22.40; 25.71; 25.90; 25.93; 28.07; 30.11; 33.83; 36.32; 39.50; 46.74; 65.65; 118.12; 118.39; 118.58; 119.72; 124.54; 128.70; 129.59; 134.37; 135.05; 135.61; 139.21; 147.14; 153.56; 193.04; 209.92. MS (relative intensity) m/z: 486 (3); 417(39); 349(100); 333(15); 295(4); 251(2); 207(4); 77(5); 69(26); 41(29). IR (cm^{-1}): 3224, 2988, 2220, 1615, 1463, 942, 962, 784. HRMS (ESI): m/z $[M + H]^+$ calcd for $C_{32}H_{43}N_2O_2$: 487.33191; found: 487.33183.

4. Conclusions

In conclusion, we synthesized 3-Isobutyl-5,5,7-tris(3-methylbut-2-en-1-yl)-1-phenyl-1,7-dihydro-4*H*-indazole-4,6(5*H*)-dione and performed a full structural elucidation of its ^1H and $^{13}C\{^1H\}$ NMR signals. This is an important contribution to produce the first results related to lupulone reactivity, which could be used for pharmacological applications. Considering the lupulone derivative **4** accessed, these results highlight the possibilities for new derivatizations, especially considering the tautomerism effect.

Supplementary Materials: The following are available online. Figures S1–S7: ^1H, ^{13}C, COSY, HSQC and HMBC spectra; Figure S8: Mechanism to access the Lupulone Derivative **1** (Expected) and Lupulone Derivative **3** (not favored).

Author Contributions: R.G.J. supervised; M.S.S. designed and conceived the experiments and wrote, reviewed and edited the manuscript; D.H. wrote, reviewed and edited the manuscript; J.E.R.d.N. developed the synthetic methodology and performed the experiments. All authors have read and agreed to the published version of the manuscript.

Funding: This research was funded by CNPq (Grants 409782/2018-1, 308015/2019-3 and 309013/2019-4) and FAPERGS (ARD 19/2551-0001258-6) and partially financed by the Coordenação de Aperfeiçoamento de Pessoal de Nivel Superior-Brasil (CAPES), Finance Code 001.

Data Availability Statement: The data presented in this study are available in the Supplementary Materials for this article.

Acknowledgments: The authors are grateful to UFPel for providing support to carry out this work and the funding agencies for the financial support. Additionally, we would like to thank the reviewers for their revisions and comments, which were useful to understand the product obtained.

Conflicts of Interest: The authors declare no conflict of interest.

References

1. Jacob, R.G.; Oliveira, D.H.; Dias, I.F.C.; Schumacher, R.F.; Savegnago, L. Óleos essenciais como matéria-prima sustentável para o preparo de produtos com maior valor agregado. *Rev. Virtual Quim.* **2016**, *9*, 294–316. [CrossRef]
2. Gallezot, P. Conversion of biomass to selected Chemical products. *Chem. Soc. Rev.* **2012**, *41*, 1538–1558. [CrossRef] [PubMed]
3. Schultz, C.; Chiheb, C.; Pischetsrieder, M. Quantification os co-, n-, and ad-lupulone in hop-based dietary supplements and phytopharmaceuticals and modulation of their contentes by the extraction method. *J. Pharm. Biomed. Anal.* **2019**, *168*, 124–132. [CrossRef] [PubMed]
4. Tyrrell, E.; Archer, R.; Tucknott, M.; Colston, K.; Pirianov, G.; Ramanthan, D.; Dhillon, R.; Sinclair, A.; Skinner, G.A. The synthesis and anticancer effects of a range of natural and unnatural hop β-accids on breast câncer cells. *Phytochem. Lett.* **2012**, *5*, 144–149. [CrossRef]
5. Goese, M.; Kammhuber, K.; Bacher, A.; Zenk, M.H.; Eisenreich, W. Biosynthesis of bitter acids in hops. A ^{13}C-NMR and ^{2}H-NMR study on the building blocks of humulone. *Eur. J. Biochem.* **1999**, *263*, 447–454. [CrossRef] [PubMed]
6. Intelmann, D.; Haseleu, G.; Hofmann, T. LC-MS/MS Quantification of Hop-Derived Bitter Compounds in Beer Using the ECHO Technique. *J. Agric. Food Chem.* **2009**, *57*, 1172–1182. [CrossRef] [PubMed]
7. Tyrrel, E.; Archer, R.; Skinner, G.A.; Singh, K.; Colston, K.; Driver, C. Structure elucidation and an investigation into in vitro effects of hop acids on human cancer cells. *Phytochem. Lett.* **2010**, *3*, 17–23. [CrossRef]
8. Bogdanova, K.; Roderova, M.; Kolar, M.; Langova, K.; Dusek, M.; Jost, P.; Kubelkova, K.; Bostik, P.; Olsovska, J. Antibiofilm activity of bioactive hop compounds humulone, lupulone and xanthohumol toward susceptible and resistant staphylococci. *Res. Microbiol.* **2018**, *169*, 127–134. [CrossRef] [PubMed]
9. Castro, M.R.; Victoria, F.N.; Oliveira, D.H.; Jacob, R.G.; Savegnago, L.; Alves, D. Essential oil of Psidium cattleianum leaves: Antioxidant and antifungal activity. *Pharm. Biol.* **2015**, *53*, 242–250. [CrossRef] [PubMed]
10. Fonseca, A.O.S.; Pereira, D.I.B.; Jacob, R.G.; Maia Filho, F.S.; Oliveira, D.H.; Maroneze, B.P.; Valente, J.S.S.; Osório, L.G.; Botton, S.A.; Meireles, M.C.A. In vitro susceptibility of Brazilian Pythium insidiosum isolates to essential oil of some Lamiaceae Family species. *Mycopathologia* **2015**, *179*, 253–258. [CrossRef] [PubMed]
11. Lenardão, E.J.; Bottesselle, G.V.; Azambuja, F.; Perin, G.; Jacob, R.G. Citronellal as key compounds in organic synthesis. *Tetrahedron* **2007**, *63*, 6671–6712. [CrossRef]
12. Montenegro, L.M.P.; Griep, J.B.; Tavares, F.C.; Oliveira, D.H.; Bianchini, D.; Jacob, R.G. Synthesis and characterization of imine-modified silicas obtained by the reaction of essential oil of *Eucalyptus citriodora*, 3-aminopropyltriethoxysilane and tetraethylorthosilicate. *Vib. Spectrosc.* **2013**, *68*, 272–278. [CrossRef]
13. Chagas, A.C.; Domingues, L.F.; Fantatto, R.R.; Giglioti, R.; Oliveira, M.C.S.; Oliveira, D.H.; Mano, R.A.; Jacob, R.G. In vitro and in vivo acaricide action of juvenoid analogs produced from the chemical modification of *Cymbopogon* spp. and *Corymbia citriodora* essential oil on the cattle tick *Rhipicephalus* (Boophilus) microplus. *Veterin. Parasit.* **2014**, *205*, 277–284. [CrossRef] [PubMed]
14. Ferraz, M.C.; Mano, R.A.; Oliveira, D.H.; Maia, D.S.V.; Silva, W.P.; Savegnago, L.; Lenardão, E.J.; Jacob, R.G. Synthesis, Antimicrobial, and Antioxidant Activities of Chalcogen-Containing Nitrone Derivatives from (*R*)-Citronellal. *Medicines* **2017**, *4*, 39. [CrossRef] [PubMed]
15. Taniguchi, Y.; Taniguchi, H.; Yamada, M.; Matsukura, Y.; Koizumi, H.; Furihata, K.; Shindo, K. Analysis of the components of hard resin in hops (*Humulus lupulus L.*) and structural elucidation of their transformation products formed during the brewing process. *J. Agric. Food Chem.* **2014**, *62*, 11602–11612. [CrossRef] [PubMed]
16. Olsovska, J.; Bostikova, V.; Dusek, M.; Jandovska, V.; Bogdanova, K.; Cermak, P.; Bostik, P.; Mikyska, A.; Kolar, M. *Humulus Lupulus* L. (Hops)—A valuable source of compounds with bioactive effects for future therapies. *Mil. Med. Sci. Lett.* **2016**, *85*, 19–31. [CrossRef]
17. Radatz, C.S.; Rodrigues, M.B.; Alves, D.; PERIN, G.; Lenardão, E.J.; Savegnago, L.; Jacob, R.G. Synthesis of 1-*H*-1,5-benzodiazepines derivatives using $SiO_2/ZnCl_2$. *Heteroat. Chem.* **2011**, *22*, 180–185. [CrossRef]
18. Pretsch, E.; Bühlman, P.; Badertscher, M. *Structure Determination of Organic Compounds, Tables of Spectral Data*, 5th ed.; Springer: Berlin/Heidelberg, Germany, 2020. [CrossRef]
19. Briggs, L.H.; Penfold, A.R.; Short, W.F. Leptospermone. Part I. *J. Chem. Soc.* **1938**, 1193–1195. [CrossRef]
20. Dybowski, M.P.; Typek, R.; Bernacik, K.; Dawidowicz, A.L. Isomerization of bitter acids during the brewing process. *Ann. Univesitatis Marie Curie-Sklodowska Lub.-Pol.* **2015**, *2*, 137–144. [CrossRef]